

Drift Transport of Helical Spin Coherence in Semiconductors

Yoji Kunihashi, Haruki Sanada, Hideki Gotoh, Koji Onomitsu, and Tetsuomi Sogawa

Abstract

Spatial transport of electron spins and their electrical manipulation are fundamental technologies in the emerging field of semiconductor spintronics, where the spin degree of freedom is used as an information carrier in a device. Images of the spatial distribution of drifting spins were obtained using Kerr rotation microscopy in a GaAs quantum well where special symmetry of the spin-orbit interaction, namely a persistent spin helix (PSH) condition, was achieved. By efficiently suppressing the spin relaxation in the PSH state, we were able to demonstrate long-distance transport of electron spins over 100 μm and electrical control of the spin precession during drift transport. In a PSH condition, the frequency of the spin precession shows significant anisotropy, reflecting the dependence of effective magnetic fields on crystal orientation. A theoretical model reproduced the spin distributions well and revealed that the spin decay length was maximized near the PSH condition. The robustness of the spin coherence with respect to the variation of transport trajectory was also confirmed by employing a time-dependent in-plane electric field perpendicular to the drift direction. Further development of this technique will advance the field of semiconductor spintronics, including the physics of spin-charge coupled systems as well as applications for future spin devices.

Keywords: spintronics, spin-orbit interaction, Kerr rotation

1. Introduction

Recent developments in electronics rely on the miniaturization and integration of electronic devices in which an electron's charge is used as an information carrier. However, device size is approaching its limit, and device performance cannot be further enhanced simply by extending existing technologies. An emerging research field known as semiconductor spintronics represents an attempt to use spin instead of charge for information processing [1–3], since this will result in lower energy consumption, higher operating speeds, and further improvement of device functionality compared with conventional charge-based devices.

The electrical control and transport of electron spins are essential techniques for realizing spintronics devices. An effective magnetic field plays an important role in controlling electron spins by electri-

cal means. In general, the asymmetry of the system (e.g., the asymmetric layer structure of a quantum well (QW) or the lack of an inversion center in crystal structures) generates an internal electric field that is converted into effective magnetic fields for the coordinate system of a moving electron [4]. This is due to a relativistic effect called a spin-orbit interaction (SOI). However, SOI is a double-edged sword with spintronic devices. Because the direction of effective magnetic fields depends on the electron momentum, multiple scattering of electrons randomizes the effective magnetic fields, resulting in undesired spin relaxation [5]. A significant difficulty in the application of electron spins to semiconductor devices is preventing spin relaxation, which limits the transport length of electron spins to the order of 10 μm in semiconductor heterostructures [6].

Currently, much attention is being focused on the suppression of spin relaxation by balancing two

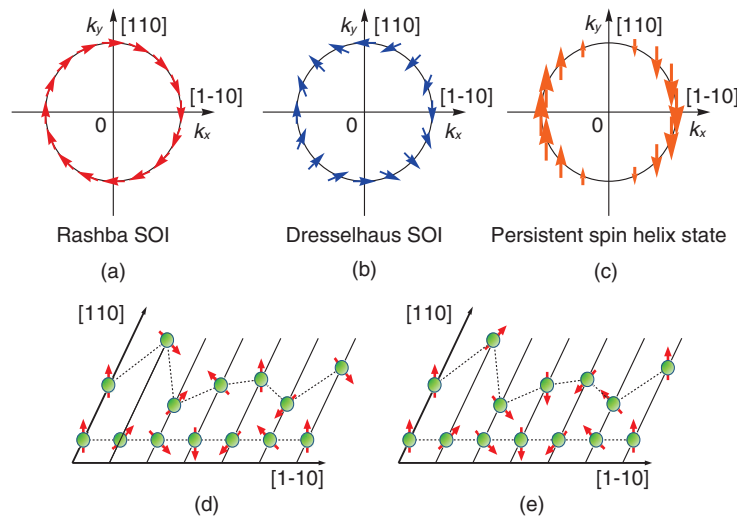


Fig. 1. Effective magnetic fields generated by (a) Rashba and (b) Dresselhaus SOIs. In (c) the persistent spin helix (PSH) state, effective magnetic fields are uniaxially oriented. Schematics of the spin relaxation caused by (d) the dependence of effective magnetic fields on momentum and (e) the coherent rotation of electron spins in the PSH state.

SOIs. In III-V semiconductor heterostructures, there are typically two kinds of SOIs. One is the Rashba SOI induced by the internal electric field in an asymmetric QW [7]. The other is the Dresselhaus SOI, which originates from the crystal field induced by the bulk inversion asymmetry in a zinc-blende crystal structure [8]. The Rashba and Dresselhaus SOIs act on electron spins as momentum-dependent magnetic fields as shown in **Figs. 1(a)** and **1(b)**. When the strengths of these two SOIs are equal, the effective magnetic field is uniaxially oriented as shown in **Fig. 1(c)**. In this condition, electron spins can precess around the same axis and do not relax even if they experience multiple scattering (**Figs. 1(d)** and **1(e)**). This special condition of SOIs is called the persistent spin helix (PSH) state, which has been theoretically predicted and experimentally confirmed [9–11]. In the PSH state, the spin transport length can be enhanced even in a system with strong SOIs.

Here, we report the spatial mapping of drifting spins in a GaAs QW where the Rashba and Dresselhaus SOIs are balanced to achieve a PSH state [12]. In the PSH state, the precession frequency of drifting spins becomes anisotropic, reflecting the crystal orientation dependence of the effective magnetic field. A comparison of experimental results and a numerical simulation based on a spin-drift diffusion model reveals that the spin decay length is maximized near the PSH condition, indicating the effective suppression of spin relaxation by the PSH state. Within the

enhanced distance of the spin transport, the transport path of electron spins can be modulated by employing time-varying in-plane voltages, suggesting the robustness of the spin coherence against geometrical variations in the spin transport.

2. Experiment

To determine a suitable structure for the PSH condition, we calculated the SOIs in a GaAs single QW structure. The Hamiltonians for the Rashba and Dresselhaus SOIs in a III-V semiconductor QW are given by

$$H_R = \alpha (\sigma_x k_y - \sigma_y k_x), \quad (1)$$

$$H_D = -\beta (\sigma_x k_y + \sigma_y k_x), \quad (2)$$

where α and β indicate the strengths of the SOIs, σ_i ($i = x, y$) is the Pauli matrix, and k_i ($i = x, y$) is the electron momentum. In this article, we defined the coordinate axis with base vectors $x \parallel [1-10]$, $y \parallel [110]$, and $z \parallel [001]$. Since the potential gradient in a QW can be modulated with an external gate voltage, the Rashba SOI parameter α is a gate-controllable value. In contrast, β is expressed by material constant γ and well thickness d in the following equation,

$$\beta = \gamma \langle k_z^2 \rangle \approx \gamma (\pi/d)^2. \quad (3)$$

According to Eq. (3), the Dresselhaus SOI is enhanced by reducing the well thickness. By solving the Poisson-Schrödinger equation, we can calculate energy

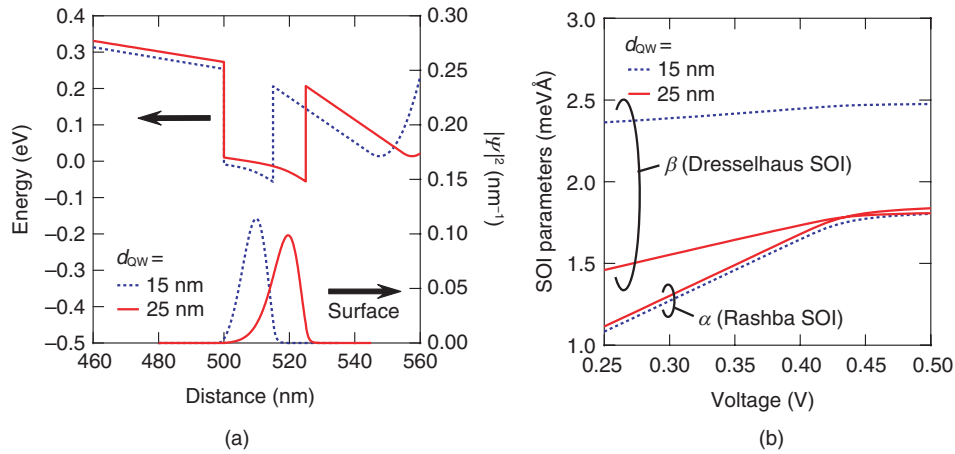


Fig. 2. (a) Energy-band profiles of the conduction band (Γ_6) in $\text{Al}_{0.3}\text{Ga}_{0.7}\text{As}/\text{GaAs}$ (15, 25 nm)/ $\text{Al}_{0.3}\text{Ga}_{0.7}\text{As}$ structures calculated with the Poisson-Schrödinger equation, whose energies are based on the position of the Fermi energy E_F . The normalized electron probability density $|\Psi|^2$ is also shown. (b) Calculated SOI parameters for 15- and 25-nm-thick QWs as functions of relative voltage, which is the relative difference between the substrate and surface potentials. The solid and dashed lines indicate the Rashba and Dresselhaus parameters, respectively.

band profiles and wave functions in the $\text{AlGaAs}/\text{GaAs}/\text{AlGaAs}$ QW structures, as shown in **Fig. 2(a)**. To confirm the contribution of the Dresselhaus SOI, we assumed two different QW thicknesses of $d = 15$ and 25 nm. The gate-voltage dependences of SOI parameters calculated by using $k \cdot p$ perturbation are shown in **Fig. 2(b)** [13]. It should be noted that the horizontal axis in Fig. 2(b) indicates the relative difference between the potentials of the surface and the substrate, which does not correspond to the experimentally applied gate voltage. In Fig. 2(b), we found that the Dresselhaus SOI parameter β depends strongly on the well thickness, whereas the Rashba SOI parameter α can be widely modulated by applying a gate voltage rather than by varying the well thickness. According to Fig. 2(b), α can be comparable to β in a 25-nm-thick QW, which indicates the possibility of the PSH condition.

Using the theoretical calculations as a basis, we designed and grew 15- and 25-nm-thick modulation-doped $\text{Al}_{0.3}\text{Ga}_{0.7}\text{As}/\text{GaAs}/\text{Al}_{0.3}\text{Ga}_{0.7}\text{As}$ single QW structures by molecular-beam epitaxy on a (001) semi-insulating GaAs substrate. The QWs were located 120 nm below the surface, and three δ -doping layers were embedded 50, 100, and 105 nm below the surface. The epitaxial wafers were fabricated into cross-shaped structures with four ohmic contacts consisting of AuGeNi layers. The central part of the structure was covered with a semi-transparent Au gate electrode as indicated in **Fig. 3(a)**.

We employed Kerr microscopy to measure the spin dynamics of the drifting electrons (**Fig. 3(b)**). Spin-polarized electrons were generated by a circularly polarized pump light. Subsequently, the spatial distribution and dynamics of the electron spins were detected with a linearly polarized probe light via the Kerr rotation angle θ_K , which was proportional to the spin density at the focused position. For a microscopic measurement of the spin coherence, the pump and probe lights were focused on the sample with 6- μm - and 3- μm -diameter spots, respectively. The temporal development of the electron spins can be observed by using a pulse laser from a mode-locked Ti:sapphire laser, whereas the steady flow of drifting spins can be measured with a continuous wave (CW) laser. All the measurements were carried out at 8 K.

3. Results and discussion

The results of time-resolved Kerr rotation microscopy for the drifting spin in a 25-nm-thick QW with the application of an in-plane electric field $V_x = 200$ mV are shown in **Fig. 3(c)**. We can see that spin-polarized electrons generated at time $t = 0$ ns move to the drain electrode. Even in the absence of an external magnetic field, we observed a spin precession resulting from the effective magnetic field induced by the SOIs. To estimate the drift velocity of the electron spins, we performed a fitting analysis on the assumption that the spatiotemporal development of drifting

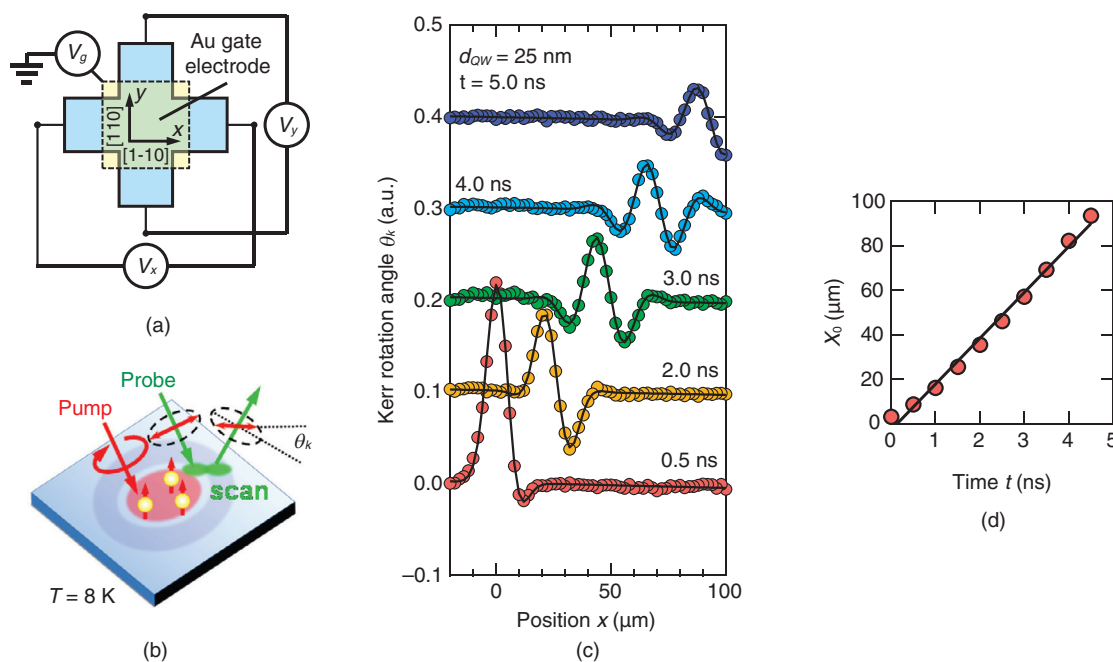


Fig. 3. (a) Schematic illustration of the top view of the sample. (b) The setup for spatially resolved Kerr rotation measurements. (c) Time-resolved Kerr rotation signal for spins drifting in a 25-nm-thick QW when applying $V_d = 200$ mV. The solid lines indicate the fitted results obtained with Eq. (4). (d) Time dependence of the displacement of a spin packet. The solid line is a linear function fitted to the experimental results.

spins can be explained by the model function,

$$\theta_K = A \exp(-(x-x_0)^2/w^2) \cos(k_{SO}(x-x_0)), \quad (4)$$

where A is the signal amplitude, x_0 and w are the displacement and width of the Gaussian, respectively, and k_{SO} is a spin wavenumber that represents the spatial frequency of the spin precession. We fitted Eq. (4) to the experimental result and extracted x_0 , which is plotted as a function of time in **Fig. 3(d)**. We found that x_0 is proportional to time t , and the slope in Fig. 3(d) indicates the drift velocity. Thus we obtained $v_d = 20.6$ km/s in a 25-nm-thick QW, which is 150 times faster than the drift velocity of the electron spins observed in bulk GaAs [14].

The spatial distribution of drifting spins in a steady state is shown in **Figs. 4(a)** and **4(b)**. In a 15-nm-thick QW, spin precession due to the effective magnetic field was observed in both the x and y directions, which reflects the isotropic strength of the effective magnetic fields. This is because the Dresselhaus SOI is dominant in the 15-nm-thick QW as predicted by a theoretical calculation. In contrast, in a 25-nm-thick QW when $V_g = -4.28$ V is applied, the precession of the drifting spins in the y direction is stopped completely, although drifting spins in the x direction pre-

cess more than five cycles in 100 μm . This strong anisotropy of the spin precession originates from the dependence of the effective magnetic field on the crystal orientation, which implies that the PSH is almost realized in a 25-nm-thick QW. Furthermore, the long-distance spin transport over 100 μm observed in the 25-nm-thick QW is attributed to the suppression of spin relaxation due to the PSH state. To determine quantitatively how close this was to the PSH condition, we performed a fitting analysis of the spatial distributions of the drifting spins. On the assumption that the contribution of the drift transport of the spins is dominant compared with spin diffusion, the spatial variation of the spin flows is given by,

$$\theta_K = A \exp(-d/\lambda_{SO}) \cos(k_{SO} d), \quad (5)$$

where d is the distance from the origin and λ_{SO} is the spin decay length. We fitted Eq. (5) to the experimental results and extracted the spin wavenumber k_{SO} . We excluded data between $d = 0$ μm and 10 μm from the fitting procedure to remove the contribution of spin diffusion. If we assume simple one-dimensional transport, the SOI parameters are proportional to the spin wavenumber,

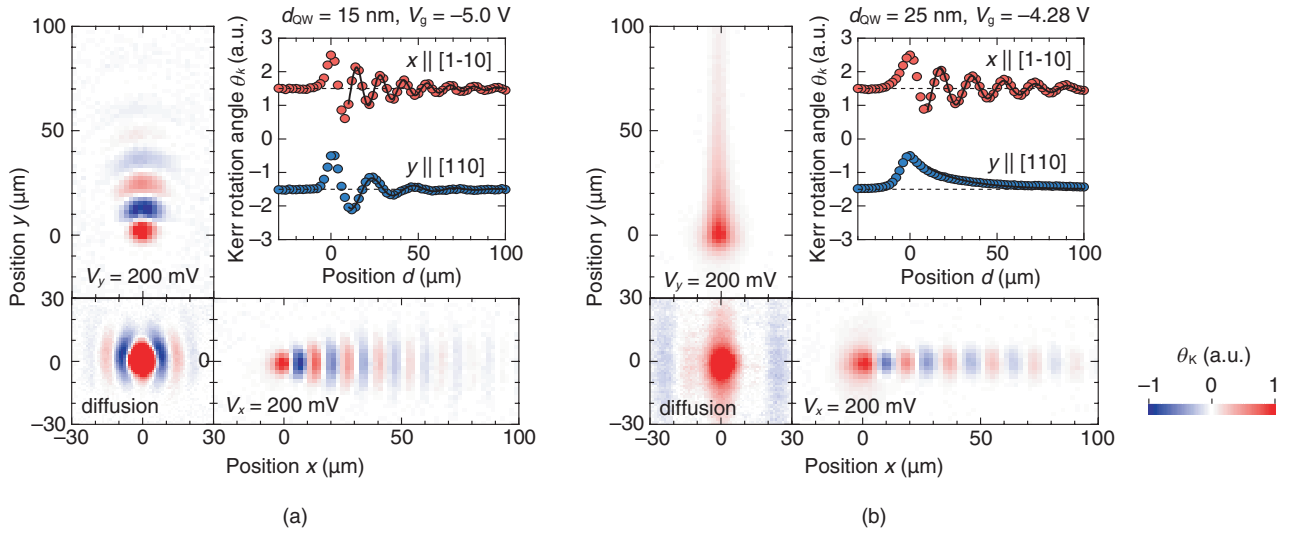


Fig. 4. (a), (b) Spatial mapping of the spin distribution for 15- and 25-nm-thick QWs. The square panels in the bottom left corners show the spin distribution for diffusive transport, while the rectangular panels are those for drift transport with in-plane electric fields. Red and blue in the maps correspond to up and down spins, respectively. The panels in the upper right corners are the cross-sectional profiles of drifting spins in the [1-10] and [110] directions. The solid lines show the fitted results obtained with Eq. (5).

$$\alpha = \frac{\hbar}{4m^*} (k_{SO}^{1-10} + k_{SO}^{1-10}), \quad (6)$$

$$\beta = \frac{\hbar}{4m^*} (k_{SO}^{1-10} - k_{SO}^{1-10}), \quad (7)$$

where m^* and \hbar are the effective mass of an electron and Planck's constant, respectively. Thus, two SOI parameters, α and β , can be estimated from k_{SO} in the [1-10] and [110] directions. The estimated SOI parameters were $\alpha = 0.58 \text{ meV\AA}$ and $\beta = 2.10 \text{ meV\AA}$ for a 15-nm-thick QW and $\alpha = \beta = 0.99 \text{ meV\AA}$ for a 25-nm-thick QW. From these results, we confirmed that the PSH state is realized in a 25-nm-thick QW.

The spatial frequency of the spin precession during drift transport is electrically controlled by the gate modulation of the Rashba SOI. The gate voltage (V_g) dependence of θ_K scanned along the [1-10] direction for $V_x = 50 \text{ mV}$ and $V_y = 0 \text{ mV}$ is shown in **Fig. 5(a)**. By varying the gate voltage, we were able to continuously modulate the spatial frequency of the drifting spin precession via gate control of the Rashba SOI. This behavior was well reproduced by a simulation based on a spin-drift-diffusion model, as shown in **Fig. 5(b)**. Assuming that the precession period in **Fig. 5(a)** depends only on α , we can compare the effect of α on the transport length by plotting spin decay length λ_{SO} versus spin wavenumber k_{SO} , where both parameters can be extracted by the fitting proce-

dure used in **Fig. 4**. The obtained λ_{SO} values are plotted as a function of k_{SO} in **Fig. 5(c)**. In both the experiment and the simulation, λ_{SO} decreases as k_{SO} diverges from the balanced condition $\alpha = \beta$, indicating that the suppression of the D'yakonov-Perel spin relaxation caused by the PSH also appears in the spin transport length.

We can transport the helical spin state along arbitrary trajectories by using a time-dependent in-plane electric field. We applied a sinusoidal ac voltage V_y^{ac} with frequency f in the y direction and dc voltages V_x^{dc} in the x direction. To excite spins at the timing of a certain phase of V_y^{ac} , the initial spins were excited with a pulsed pump light from a mode-locked laser whose repetition frequency was synchronized with f or $f/2$, whereas the Kerr signal was detected with a probe light from a CW laser. When a sinusoidal voltage was applied in a transverse direction to the drift spin transport, a clear spin flow along a winding path was observed (**Fig. 6**). The stripe patterns in the spin packet are maintained regardless of the transport trajectories. This is because in a PSH condition, spins always precess in an x - z plane, and the precession phase depends only on x [9, 10]. For all transport paths, the spin phase was conserved even at distances much longer than the precession periods, and thus, the technique will be beneficial for further exploitation of the SOI in drift spin manipulation.

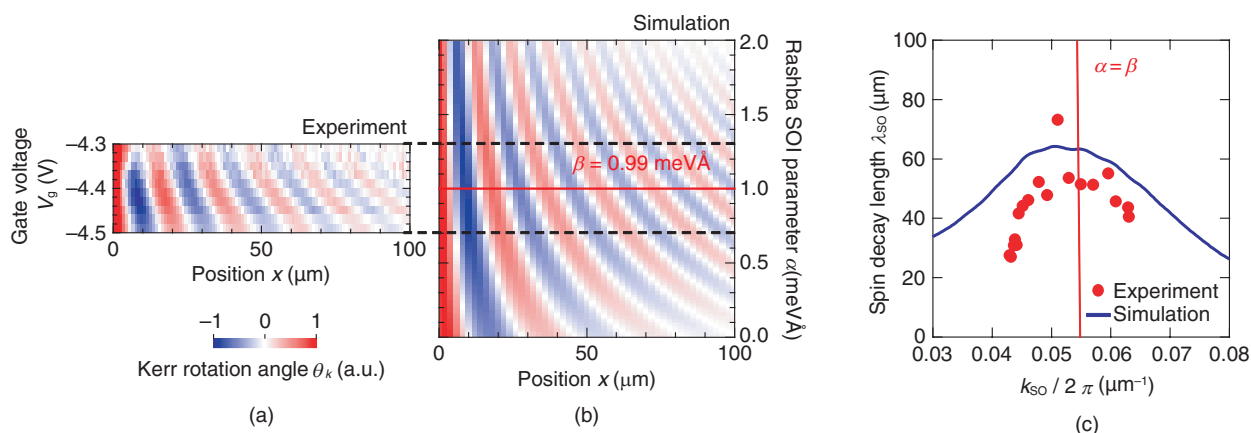


Fig. 5. SOI dependence of spin dynamics of drifting spins. (a), (b) Comparison of experimental and simulated spin distribution driven by $V_x = 50$ mV in the x direction. In the simulation, we directly varied the Rashba SOI parameters α , and the spin distribution is shown as a function of α , whereas the experimental data are plotted as a function of the gate voltage, which modulates the Rashba SOI. Note that the gate voltage shown in this figure does not correspond to that in Fig. 2. (c) Spin decay length as a function of spin wavenumber.

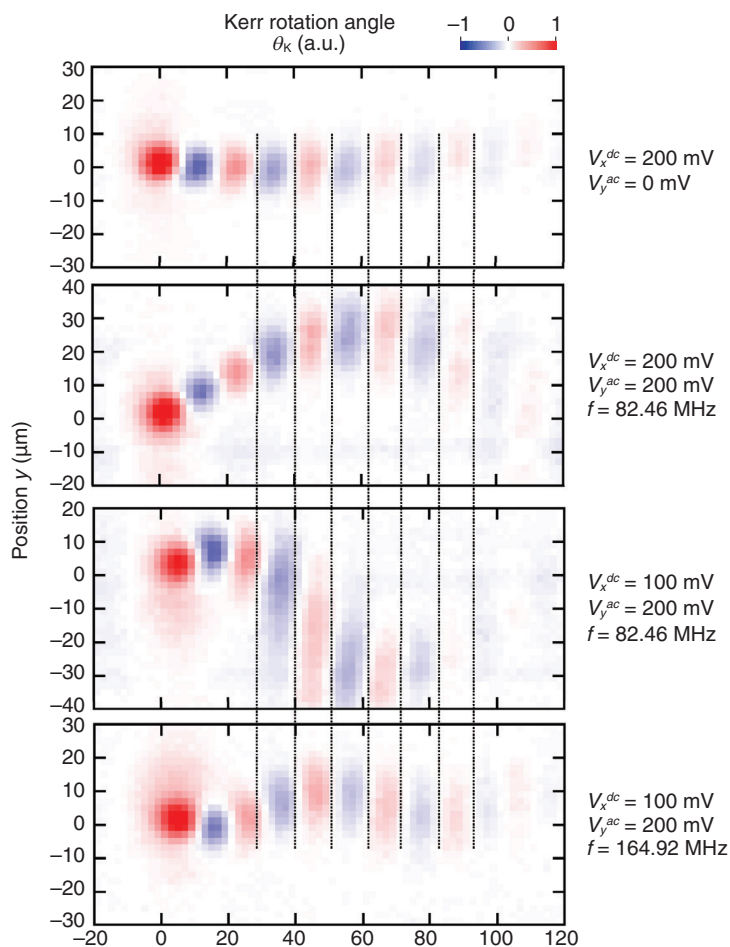


Fig. 6. Dynamic modulation of the transport path of drifting spins. Drift spin transport with a sinusoidal voltage applied in the y direction. The dc voltage V_x^{dc} and the sinusoidal voltage V_y^{ac} are specified in each figure.

4. Conclusion

The spatial distribution of drifting spins in a GaAs QW where two types of SOI, namely the Rashba and Dresselhaus SOIs, are balanced to realize a PSH state, was mapped by using temporally and spatially resolved Kerr rotation microscopy. In the PSH state, spins drifting in a direction where there are strong effective magnetic fields exhibit a fast spin precession, whereas the spin precession of spins drifting in an orthogonal direction is completely stopped. The spin decay length is maximized near the PSH condition, indicating the effective suppression of spin relaxation by the PSH state. Furthermore, we demonstrated drift spin transport over 100 μm , where the precession frequency was controlled by an external gate voltage. The results presented here show that spin coherence with a balanced SOI can be efficiently transferred to a distant place. We confirmed the robustness of the spin phase for the variation of transport paths in the PSH state. If the PSH condition is sufficiently maintained, we may also manipulate the spin states by using the gate bias voltage or a trajectory-controlled quantum operation. Further development of this technique will advance the field of semiconductor spintronics, including the physics of spin-charge coupled systems as well as applications for future spin devices.

Acknowledgments

We thank P. V. Santos of Paul-Drude-Institut für Festkörperelektronik, Berlin, Germany, and J. Nitta and M. Kohda of the Department of Materials Science, Tohoku University, Sendai, for their useful technical advice. This work was partly supported by

the Japan Society for the Promotion of Science (JSPS).

References

- [1] S. Datta and B. Das, "Electronic Analog of the Electro-optic Modulator," *Appl. Phys. Lett.*, Vol. 56, No. 7, p. 665, 1990.
- [2] S. A. Wolf, D. D. Awschalom, R. A. Buhrman, J. M. Daughton, S. von Molnár, M. L. Roukes, A. Y. Chtchelkanova, and D. M. Treger, "Spintronics: A Spin-based Electronics Vision for the Future," *Science*, Vol. 294, pp. 1488–1495, 2001.
- [3] J. Wunderlich, B.-G. Park, A. C. Irvine, L. P. Zárbo, E. Rozkotová, P. Nemeč, V. Novák, J. Sinova, and T. Jungwirth, "Spin Hall Effect Transistor," *Science*, Vol. 330, pp. 1801–1804, 2010.
- [4] R. Winkler, "Spin-orbit Coupling Effects in Two-dimensional Electron and Hole Systems," *Springer Tracts in Modern Physics*, Vol. 191, Springer, Berlin, 2003.
- [5] M. I. D'yakonov and V. I. Perel', "Spin Relaxation of Conduction Electrons in Noncentrosymmetric Semiconductors," *Sov. Phys. Solid State*, Vol. 13, pp. 3023–3026, 1972.
- [6] L. Yang, J. D. Koralek, J. Orenstein, D. R. Tibbetts, J. L. Reno, and M. P. Lilly, "Doppler Velocimetry of Spin Propagation in a Two-dimensional Electron Gas," *Nature Phys.*, Vol. 8, pp. 153–157, 2012.
- [7] Y. A. Bychkov and E. I. Rashba, "Oscillatory Effects and the Magnetic Susceptibility of Carriers in Inversion Layers," *J. of Physics C: Solid State Physics*, Vol. 17, No. 33, pp. 6039–6045, 1984.
- [8] G. Dresselhaus, "Spin-orbit Coupling Effects in Zinc Blende Structures," *Phys. Rev.*, Vol. 100, No. 2, pp. 580–586, 1955.
- [9] J. Schliemann and D. Loss, "Anisotropic Transport in a Two-dimensional Electron Gas in the Presence of Spin-orbit Coupling," *Phys. Rev. B*, Vol. 68, p. 165311, 2003.
- [10] B. A. Bernevig, J. Orenstein, and S.-C. Zhang, "Exact SU(2) Symmetry and Persistent Spin Helix in a Spin-orbit Coupled System," *Phys. Rev. Lett.*, Vol. 97, p. 236601, 2006.
- [11] J. D. Koralek, C. P. Weber, J. Orenstein, B. A. Bernevig, S.-C. Zhang, S. Mack, and D. D. Awschalom, "Emergence of the Persistent Spin Helix in Semiconductor Quantum Wells," *Nature*, Vol. 458, pp. 610–613, 2009.
- [12] Y. Kunihashi, H. Sanada, H. Gotoh, K. Onomitsu, M. Kohda, J. Nitta, and T. Sogawa, "Drift Transport of Helical Spin Coherence with Tailored Spin-orbit Interactions," *Nature Communications*, Vol. 7, p. 10722, 2016.
- [13] Th. Schäpers, G. Engels, J. Lange, Th. Klocke, M. Hollfelder, and H. Lüth, "Effect of the Heterointerface on the Spin Splitting in Modulation Doped $\text{In}_x\text{Ga}_{1-x}\text{As}/\text{InP}$ Quantum Wells for $B \rightarrow 0$," *J. Appl. Phys.*, Vol. 83, p. 4324, 1998.
- [14] J. M. Kikkawa and D. D. Awschalom, "Lateral Drag of Spin Coherence in Gallium Arsenide," *Nature*, Vol. 397, pp. 139–141, 1999.



Yoji Kunihashi

Research Scientist, Quantum Optical Physics Research Group, Optical Science Laboratory, NTT Basic Research Laboratories.

He received a B.E., M.E., and Ph.D. in electrical engineering from Tohoku University, Miyagi, in 2007, 2009, and 2012. He joined NTT Basic Research Laboratories in 2012. His research interests include the optical and electrical properties of low-dimensional semiconductor nanostructures, spin-related phenomena in solid-state materials, and fabrication technology of semiconductor/insulator/metal hybrid nanostructures. He is a member of the Japan Society of Applied Physics (JSAP).



Haruki Sanada

Research Scientist, Distinguished Researchers, Quantum Optical Physics Research Group, Optical Science Laboratory, NTT Basic Research Laboratories.

He received a B.E., M.E., and Ph.D. in electrical engineering from Tohoku University, Miyagi, in 2001, 2002, and 2005. He joined NTT Basic Research Laboratories in 2005. His research interests include the optical properties of low-dimensional semiconductor nanostructures and carrier spin dynamics modulated by surface acoustic waves and their application to solid-state quantum information processing. He is a member of JSAP.



Hideki Gotoh

Executive Manager of Research Planning Section, General Manager of Optical Science Laboratory, and Group Leader of Quantum Optical Physics Research Group, NTT Basic Research Laboratories.

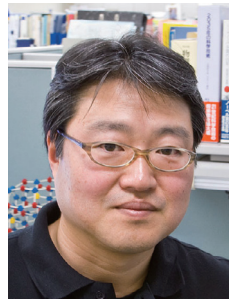
He received a B.E., M.E., and Ph.D. in engineering from Hiroshima University in 1991, 1993, and 2000. Since joining NTT Basic Research Laboratories in 1993, he has been working on optical physics and device applications of semiconductor nanostructures. He is a member of JSAP and the Optical Society of America.



Koji Onomitsu

Senior Research Scientist, Low-Dimensional Nanomaterials Research Group, Materials Science Laboratory, NTT Basic Research Laboratories.

He received a B.E. and M.E. in electrical engineering from Aoyama Gakuin University, Tokyo, in 1998 and 2000, and a Ph.D. in electrical engineering from Waseda University, Tokyo, in 2004. He joined NTT Basic Research Laboratories in 2006. His current interests are crystal growth and device applications of two-dimensional layered materials such as MoSe₂. He is a member of JSAP.



Tetsuomi Sogawa

Director of NTT Basic Research Laboratories.

He received a B.E., M.E., and Ph.D. in electrical engineering from the University of Tokyo in 1986, 1988, and 1991. He joined NTT Basic Research Laboratories in 1991. From 2004 to 2006, he worked for the Council for Science and Technology Policy, Cabinet Office, Japan, as a deputy director for policy planning. His current research interests include fabrication technology for low-dimensional nanostructures, optical properties of quantum dots/wires and photonic crystals, spin-related phenomena, and SAW application to nanostructures. He is a member of JSAP.